2015

BERYLLIUM NITRATE SUPPORTS FIBROBLAST MIGRATION AS AN ESSENTIAL COMPONENT OF SKIN AND LIMB REGENERATION IN AXOLOTLS

Adam Boyd Cook
University of Kentucky, abcook217@uky.edu

STUDENT AGREEMENT:

I represent that my thesis or dissertation and abstract are my original work. Proper attribution has been given to all outside sources. I understand that I am solely responsible for obtaining any needed copyright permissions. I have obtained needed written permission statement(s) from the owner(s) of each third-party copyrighted matter to be included in my work, allowing electronic distribution (if such use is not permitted by the fair use doctrine) which will be submitted to UKnowledge as Additional File.

I hereby grant to The University of Kentucky and its agents the irrevocable, non-exclusive, and royalty-free license to archive and make accessible my work in whole or in part in all forms of media, now or hereafter known. I agree that the document mentioned above may be made available immediately for worldwide access unless an embargo applies.

I retain all other ownership rights to the copyright of my work. I also retain the right to use in future works (such as articles or books) all or part of my work. I understand that I am free to register the copyright to my work.

REVIEW, APPROVAL AND ACCEPTANCE

The document mentioned above has been reviewed and accepted by the student's advisor, on behalf of the advisory committee, and by the Director of Graduate Studies (DGS), on behalf of the program; we verify that this is the final, approved version of the student's thesis including all changes required by the advisory committee. The undersigned agree to abide by the statements above.

Adam Boyd Cook, Student

Dr. Ashley W. Seifert, Major Professor

Dr. David Westneat, Director of Graduate Studies

BERYLLIUM NITRATE SUPPORTS FIBROBLAST MIGRATION AS AN ESSENTIAL COMPONENT OF SKIN AND LIMB REGENERATION IN AXOLOTLS

THESIS

A thesis submitted in partial fulfillment of the requirements for the degree of Master of Biological Science in the Department of Biology at the University of Kentucky.

By

Adam Boyd Cook

Lexington, Kentucky

Director: Dr. Ashley W. Seifert, Professor of Regeneration Biology

Lexington, Kentucky

2015

ABSTRACT OF THESIS

BERYLLIUM NITRATE SUPPORTS FIBROBLAST MIGRATION AS AN ESSENTIAL COMPONENT OF SKIN AND LIMB REGENERATION IN AXOLOTLS

Tissue regeneration in salamanders is a robust process that is not easily interrupted or altered. Therefore, inhibiting regeneration provides a means to interrogate the underlying cellular and molecular mechanisms regulating this complex event. Here we show that application of a relatively low concentration of beryllium nitrate solution (100mM) causes a delay in skin regeneration and severely alters normal limb regeneration. We provide evidence showing a beryllium-induced reduction in dermal fibroblast migration *in vivo* and *in vitro*. We link this phenomenon to delayed regeneration of the skin and abnormal blastema formation resulting in limb patterning defects during regeneration. Though our results show a slight reduction in fibroblast proliferation during the early stages of limb regeneration, we attribute this to an overall reduction in fibroblast presence at the site of injury. Keratinocytes appeared unresponsive to beryllium treatment with the rates of re-epithelialization and proliferation not significantly different between treatment and control groups. Taken together, these data reinforce a necessary role for fibroblasts during tissue regeneration and show that beryllium nitrate inhibits normal fibroblast behavior.

KEYWORDS: Beryllium Nitrate, Fibroblast Migration, Mexican Axolotl, Regeneration, Histology

Adam Boyd Cook

November 17, 2015

BERYLLIUM NITRATE SUPPORTS FIBROBLAST MIGRATION AS AN ESSENTIAL COMPONENT OF SKIN AND LIMB REGENERATION IN AXOLOTLS

By

Adam Boyd Cook

Ashley Seifert
Director of Thesis

David Westneat
Director of Graduate Studies

November 17, 2015

ACKNOWLEDGMENTS

The following thesis, while considered an individual work, was sculpted and improved by the input of multiple talented individuals. I would first like to acknowledge my Committee Chair, Dr. Ashley Seifert for the mentorship he provided throughout my two and a half year residence and the challenge to go above and beyond what was expected. Additionally, the valuable feedback of Committee Member Dr. Jeramiah Smith and Dr. Randal Voss was instrumental in guiding experimental design and interpretation of the data contained within. I would also like to thank Committee Member Dr. Bruce O'Hara for volunteering to serve on my committee on such short notice and contributing to the success of my defense.

In addition to the administrative support, I received technical assistance from multiple individuals in the field of regeneration. I offer my thanks to Drs. Karen Escheverri, Stephanie Roy, and Edmund Rucker for techniques and resources for cellular culture. I also could not have completed the statistical analysis of the data without the expertise of Dr. Anthony Attophzhy and Kevin Kump.

Lastly, I would like to thank my mother Penelope Boyd-Gear and stepfather Mark Gear for their patience, their advice to work hard, and their insistence to be the best scientist that I can be.

TABLE OF CONTENTS

LIST OF TABLES

LIST OF FIGURES

CHAPTER 1

INTRODUCTION

Salamanders and newts are unique among tetrapods for their almost limitless ability to regenerate complex tissues and organs, including an entire limb (Butler and Ward, 1967; Eguchi et al., 2011; Wallace, 1981). Amazingly, this ability is not restricted to a single regeneration event as repeated bouts of newt limb amputation continuously produce new limbs (Spallanzani, 1769). This example underscores the robust nature of regeneration and hints at the importance of local cells to continually divide and supply the raw material to faithfully restore a functional limb. Limb regeneration in salamanders and newts represents an example of epimorphic regeneration whereby cell proliferation precedes morphogenesis to restore the missing appendage. As cells aggregate at the injury site they form a blastema, a transient mass of lineage restricted progenitor cells. Both blastema formation and blastemal cell proliferation are absolutely required for successful regeneration following limb amputation.

Despite the robust nature of epimorphic regeneration, a few techniques can be employed to significantly alter and even completely inhibit regeneration of the limb. There are three classically defined ways to inhibit appendage regeneration: (1) severing the nerve supply, (2) disrupting positional information and (3) inhibiting cell proliferation. Examples of nerve dependence can be seen in early regeneration studies on amphibians. When nerves were severed prior to an amputation of the limb, a blastema failed to develop and regeneration would not occur until the nerve supply had been restored (Brockes, 1987; Schotté and Butler, 1941; Singer, 1951; Todd, 1823). While effective, the effect of denervation is not permanent since neurons regrow into the limb

stump a short time after the procedure. Re-amputation of a previously denervated limb will lead to normal regeneration (Salley and Tassava, 1981).

Dermal fibroblasts play a fundamental role during blastema formation and contain essential patterning information required for limb regeneration (Bryant and Gardiner, 1989; Bryant et al., 2002a; Bryant et al., 2002b; Gardiner et al., 1986; Lheureux, 1975b; Muneoka et al., 1986). Following an injury and peak inflammatory response, fibroblasts migrate to the wound site, interact locally, and deposit extracellular matrix (ECM), which directs cellular proliferation and migration (Calve et al., 2010; Seifert et al., 2012). The interaction of cells from different circumferential locations is absolutely required for proper blastema formation (Carlson, 1974; Lheureux, 1975a; Lheureux, 1975b). Disturbing this pattern by perturbing the normal dorsal-ventral, anterior-posterior, or proximal-distal axes can cause aberrations in regeneration ranging from supernumerary limbs to the complete inhibition of regeneration (Bryant, 1976; Slack, 1983). Proliferation, outgrowth, and differentiation of cells within the blastema formalize their positional identities, establishing the future pattern of the new limb.

Various chemical and molecular inhibitors have been used to probe the mechanisms that contribute to regeneration in salamanders. Examples include colchicine, LE135, Chloramphenicol, and Actinomycin D to name a few (Burnet and Liversage, 1964; Carlson, 1967, 1969; Del Rincon and Scadding, 2002; Thornton, 1943). Retinoic acid (RA) treatment can proximalize limb stump cells in salamanders and newts, inducing regeneration of a full limb (e.g., zeugopod, stylopod and autopod) from a distal plane of amputation (Maden et al., 1985). The absence of RA during limb regeneration completely inhibits regeneration, as shown by the application of the retinoid antagonist

LE135 (Del Rincon and Scadding, 2002). The mechanism for this phenomenon has been previously elucidated, with RA treatment upregulating the expression of homeobox gene *Meis1*, normally expressed proximally in the developed limb (Qin et al., 2002). Overexpression of *Meis1* in distal cells results in proximalization of affected cells in the absence of RA (Mercader et al., 1999). Exposing axolotl epidermis to Actinomycin D temporarily inhibits regeneration by delaying the formation of the apical ectodermic cap (Carlson, 1969). Actinomycin D was later revealed to inhibit RNA transcription by binding to DNA and hindering RNA polymerase during elongation (Sobell, 1985). Chloramphenicol is a powerful antibiotic that has been used for over half a century. It is also known for its potential adverse effects on the patient, most notably its damaging effect on mitochondria (Yunis, 1989). In fact, treating *Notopthalmus viridescens* with chloramphenicol is sufficient to inhibit limb regeneration (Burnet and Liversage, 1964). Thornton (1943) demonstrated that Colchicine can inhibit limb regeneration in larval salamanders, and this was later shown to result from Colchicine-induced nerve damage and inhibited cellular proliferation (Singer et al., 1956). In some cases, these compounds had toxic side effects on the entire organism, broadly inhibited cellular processes, or negatively impacted cell proliferation.

In 1949, Charles S. Thornton demonstrated that briefly exposing newly amputated limbs to the alkaline earth metal beryllium, a compound not utilized by living organisms in basic cellular functions, completely inhibited limb regeneration in juvenile marbled salamanders (*Ambystoma opacum*). Using contralateral limbs as control, the beryllium-exposed limbs did not regenerate, whereas the contralateral limb regenerated normally. Beryllium was the only element of the alkali metal and alkaline earth metal groups shown

to inhibit regeneration, as Needham (1941) tested multiple elemental compounds of similar grouping on the periodic table and found that no other metal could inhibit regeneration at the same exposure time and concentration. Even lithium, an element very similar to beryllium, had only a minor impact on regeneration and only at much higher concentrations and exposures. One recent study in *Xenopus* suggested that beryllium acts as a potent mediator of inflammation to inhibit larval limb regeneration and another study suggested that beryllium inhibits cellular function by antagonizing the PIP3 inositol pathway (Mescher et al., 2013; Tsonis et al., 1991). In light of these studies, and with the mechanism of beryllium inhibition of regeneration still a mystery, we asked whether beryllium nitrate might affect the immune response to injury, cell proliferation, death and migration.

We used the axolotl (*Ambystoma mexicanum*) to explore the underlying basis of beryllium inhibition of regeneration. Using a full-thickness excisional skin wound model (Seifert et al., 2012) and classic limb amputations we show that beryllium exposure dose not increase immune cell infiltration or increase cell death. Instead, using *in vivo* and *in vitro* techniques we show that beryllium inhibits axolotl fibroblast migration and that this affects extends to human fibroblasts as well without a concomitant increase in cell death. Surprisingly, we find that limb regeneration in the axolotl is not completely inhibited, and that beryllium exposure delays, rather than inhibits, skin regeneration.

METHODS

Animals

Ambystoma mexicanum (Mexican axolotl) were acquired from the Ambystoma Genetic Stock Center (AGSC, Lexington, KY) or from our laboratory colony. Animals were housed individually in an aquatic flow-through system at 17-18˚C in modified Holtfreter's Solution and maintained on California blackworms (*Lumbriculus variegatus*, J.F. Enterprises, Oakdale, CA). All procedures were conducted in accordance with, and approved by, the University of Kentucky Institutional Animal Care and Use Committee (IACUC Protocol: 2013-1174).

Full-thickness Excisional (FTE) Wounding and Limb Amputations

Adult axolotls were anesthetized by full submersion in Benzocaine (Sigma-Aldrich, St. Louis, MO) 0.01% (aqueous). Sterile 4mm biopsy punches (Sklar Instruments, West Chester, PA) were used to create full thickness epithelium (FTE) wounds through the skin into the dorsal muscle. Four wounds were created per animal on the dorsal surface posterior to the forelimbs and anterior to the hindlimbs. In order to harvest wound tissue at specific time-points, animals were anesthetized as above and the entire wound was harvested by cutting around the wound with iridectomy scissors. For limb amputations, each limb was amputated through the lower humerus of the forelimbs perpendicular to the limb with scissors. The protruding bone was trimmed to the stump to aid wound closure and regeneration. The regenerating limb was harvested by amputating just proximal to the original cut site. The left limb and left FTE wound always served as the experimental group, while the right always served as the control. Skin wounds were harvested at particular time points post injury based on our previous

analysis of skin regeneration in axolotls (Seifert et al., 2012). Limbs were harvested according to well-established morphological stages of regeneration (Wallace, 1981).

Beryllium Nitrate (BeN) Treatment

A 100mM working stock of beryllium nitrate was prepared by diluting a stock solution (35% w/v) (Sigma-Aldrich) in distilled water. Following a single limb amputation or FTE wound, animals were placed in 100mM BeN for 2 minutes, after which they were continually rinsed in running tap water for 10 minutes. After rinsing in water, either the contralateral limb or a second wound corresponding to the mirror position across the dorsal midline was made and the injuries were allowed to regenerate. In this way, each animal served as its own control. For *in vitro* experiments, three dilutions of BeN were prepared (1mM, 10mM and 100mM) and tested for cytotoxicity. Cytotoxicity and cell death was assessed using the vital dye Trypan Blue. Based on these tests 10mM BeN was used in all subsequent cell culture experiments.

Histology and Immunohistochemistry

Harvested tissues were fixed in 10% neutral buffered formalin (NBF) (American Master Tech Scientific Inc., Lodi, CA) overnight (~16-24hr), washed in phosphate buffered saline (PBS) (MP Biomedicals LLC, Santa Ana, CA) 3 times, and dehydrated in 70% EtOH. Samples were stored in 70% EtOH at 4˚C until being processed for paraffin embedding. Limb samples were decalcified in 10% EDTA (pH 7.4) for 3 days at room temperature with daily changes before processing. All tissue processing was completed at the University of Kentucky using a rapid microwave histoprocessor (Milestone Medical Technologies, Kalamazoo, MI). Tissue was embedded in paraffin (Leica

Biosystems, Buffalo Grove, IL) and 5 µm sections were placed onto Superfrost Plus slides (Fisher Scientific). Tissue sections were processed for routine histology and stained with Masson's trichrome (Richard-Allen Scientific, Kalamazoo, MI), Picrosirius Red (American Master Tech) or Alcian Blue (Sigma-Aldrich). For frozen sections, samples were fixed for 1 hour in 10% NBF at 4˚C, washed in PBS, equilibrated in 30% sucrose and OCT freezing medium, and rapidly frozen on dry ice to be stored at -20ºC. Frozen sections where cut at 12µm.

For general immunohistochemistry preparation, slides were deparaffinized, rehydrated and antigen retrieval was performed if necessary (see below for each antibody). Sections were then washed in tris-buffered saline (TBS), blocked for biotin and streptavidin at 15 minute intervals each (Vector Labs Inc., Burlingame, CA), and incubated with 1˚ antibody (see below) overnight at 4˚C. Isotyped IgGs matching the primary antibody were run as negative controls. The following day, slides were washed in TBS, incubated with biotinylated 2˚ antibody (Vector Labs) for 30 minutes and subsequently incubated with streptavidin conjugated horseradish peroxidase antibody (Vector Labs) for 30 minutes. The antibodies were visualized using DAB (3,3-diaminobenzidine) (Vector Labs) or incubated with a streptavidin conjugated Alexa-Flour 594 (Invitrogen, Carlsbad, CA). Nuclei were counterstained with either 10µg/ml Hoescht (Invitrogen) for fluorescence or Mayer's hematoxylin for bright field visualization. Coverslips were mounted using either ProLong Gold mounting medium (Invitrogen) for fluorescence or Cytoseal XYL (Thermo-Fisher) for bright field visualization.

For BrdU immunohistochemistry, a 3% hydrogen peroxide in methanol block was applied for 10 minutes prior to rehydration of the deparaffinized sections. Slides were incubated in a 2M HCl solution at 37ºC for 15 minutes and rinsed 4 times in distilled water. Reagents A (Avidin DH) and B (Biotinylated Horseradish Peroxidase H) from the Vectastain ABC kit (Vector Labs) were mixed in a 1:1 ratio of A:B at a concentration of 20µL of each reagent per mL TBS after the application of the biotinylated 2º antibody. Each slide was treated with this mixture for 30 minutes. After a TBS rinse, reagents from the DAB substrate kit (Vector Labs) were mixed according to the kit instructions (1 drop buffer solution, 2 drops DAB stock solution, 1 drop hydrogen peroxide solution, in 2.5mL distilled water). The mixture was applied to each slide individually, observed through a microscope, and timed for consistency among samples. The reaction was immediately quenched in distilled water once time elapsed. Slides were counterstained with Mayer's hematoxylin for 10 seconds and rinsed in distilled water. All slides were dehydrated to 100% EtOH, cleared in xylenes, and mounted using Cytoseal XYL.

For EdU immunohistochemistry, sections were deparaffinized and rehydrated in TBS prior to treatment with EdU labeling reagents. Each slide was incubated in the dark for 30 minutes with 220µL of an EdU-labeling master mix consisting of 11µL of 2M Tris at pH 8.5, 4.4µL of 50mM copper(II) sulfate, 0.44µL of Alexafluor azide (Invitrogen) at 0.5mg/mL, 44µL of 0.5M ascorbic acid, and 160.6µL of ddH_2O. After a rinse with TBS, sections were exposed to 1µg/mL Hoescht for 5 mins in the dark, rinsed for 5 mins with ddH_2O, and mounted with ProLong Gold.

Antibodies

For paraffin sections; L-plastin (gift of P. Martin) 1:2000, Tenascin-c (Millipore, AB19013), anti-BrdU (Accurate Scientific) 1:500, and Collagen I (Rockland Inc., Limerick, PA) 1:500, *Ambystoma* fibronectin (gift of Thierry Darribere) 1:300. Antigen retrievals used were; microwave and citrate buffer (pH. 6.0) (L-plastin, Tenascin-c, anti-BrdU) for 20 minutes or proteinase K treatment (DAKO) for 2 minutes (collagen type I, fibronectin). Negative controls were run using appropriate IgGs at the same concentration as the 1˚ antibody. A GFP filter was used to detect autofluorescing erythrocytes.

Analysis of Cell Death and Proliferation

Cells undergoing apoptosis were detected using a TUNEL assay employing a GFP tag (Roche Life Sciences, Indianapolis, IN). A cell death index was calculated for dermal cells expressing GFP divided by the total number of cells (stained with Hoescht) present in the same counting field.

To detect cells that transitioned through S-phase, 100mg/kg BrdU was IP injected into axolotls and tissues were harvested after 24 hours. Detection was carried out on formalin-fixed, paraffin embedded tissue sections. After sectioning, sections were deparaffinized, blocked for endogenous peroxidase activity (see DAB immunohistochemistry above), rehydrated, antigen retrieved using pH 6.0 sodium citrate buffer in a rapid microwave histoprocessor (Micron Instruments, Inc. Carlsbad, CA) for 20 minutes, rinsed thoroughly in water and placed in TBS. The standard horseradish peroxidase visualization protocol was then followed (see DAB immunohistochemistry above). Further detection of S-phase transition was conducted with 10µg/g EdU, which

was IP injected into axolotls as described above. Samples were harvested after 24 hours, formalin fixed, paraffin embedded, and sectioned. The fluorescent visualization protocol was then followed (see EdU immunohistochemistry above).

GFP Tissue Transplantations

To track dermal fibroblasts *in vivo*, full-thickness skin comprising dermis and epidermis was extracted from the dorsal flank of axolotls constitutively expressing GFP (n=5 individuals per group) in all cell types (see Figure 6A). Identical injuries were made on wild type (WT) individuals of approximate age and size. Two wounds were made on WT animals at least 1cm apart, one for treatment with BeN and the other as a control. A GFP tissue graft was placed into the open wound on WT animals and attached with Vetbond (3M, Saint Paul, MN). Wounds were allowed to heal and integrate with host tissue for 2 weeks. After 2 weeks, a second injury was made in the center of the 8mm GFP transplant using a 4mm biopsy punch. The anterior-most transplant of each animal was injured first and treated with 100mM BeN for 2 minutes followed by a 10-minute rinse (see BeN treatment above). A biopsy was taken from the remaining transplant and this wound served as the control. Each transplant was harvested 14 days later using an 8mm biopsy punch and preserved for cryosectioning. Using this methodology, GFP+ cells in the wound bed were expected to represent fibroblasts because: (1) GFP epidermis in the original donor tissue was covered and replaced by host WT epidermis, (2) circulating host blood and immune cells were not GFP+, and (3) the majority of fibroblast cells are locally derived from a 200-500µm area immediately surrounding the injury (Mchedlishvili et al., 2007), which constitutively expressed GFP.

Microscopy and Image Acquisition

Bright-field images were taken on a BX53 light microscope (Olympus, Tokyo, Japan) using a DP80 CCD camera (Olympus). Whole mount images were taken on an SZX10 light microscope (Olympus) using a DP73 CCD camera (Olympus). All *in vitro* plate images were taken on an IX71 inverted microscope (Olympus) with a DP72 CCD camera (Olympus). Tissue from a minimum of three individuals was used for quantitative data.

Circular Scratch Assays

Two cell types were analyzed *in vitro*: human adult dermal fibroblasts (hADF) (gift of Karen Escheveri, acquired from Lonza Group Ltd., Walkersville, MD) and axolotl fibroblasts (AL1) (gift of Stephanie Roy). Both cell types were expanded in T-25 and T-75 cell culture flasks (Greiner Bio-One, Monroe, NC). AL1 cells were grown in a media containing 60% L-15 (Leibovitz) Medium without L-glutamine (Sigma-Aldrich), 32% ddH_2O, 5% fetal bovine serum (FBS) (GE Healthcare Bio-Sciences, Pittsburgh, PA), 1% insulin/selenium/transferrin (Life Technologies, Grand Island, NY), 1% penicillin/streptomycin/amphotericin-b (Sigma-Aldrich), and 1% L-glutamine (Life Technologies). The hADF cells were grown in a media containing 88% Dulbecco's Modified Eagle Medium/F-12 (DMEM) (Life Technologies) 10% FBS (GE Healthcare Bio-Sciences), 1% insulin/selenium/transferrin (Life Technologies), 1% penicillin/streptomycin/amphotericin-b (Sigma-Aldrich). Cells were passaged at 70-80% confluency. Cells were passaged by rinsing with Dulbecco's PBS solution (DPBS) (Life Technologies), treating with 0.25% Trypsin-ETDA (Life Technologies) for 3-5 minutes, and centrifuging for 3 minutes at 3000rpm. Each cell line was split 1:2 or 1:3 into new

flasks with fresh media until a large stock of cells was obtained. Additional cells were slowly frozen in media with 10% DMSO at -80ºC and stored long-term in liquid nitrogen. Both cell types were grown in 12-well tissue culture treated plates and allowed to reach ~80% confluency prior to any procedure. Half of the wells were treated with 10mM beryllium nitrate and rinsed 3 times with DPBS. Cells were then scraped off with a cotton tip applicator in the very center of each well. Images were taken every 12 or 24 hours up to 96 hours (hADF cells) or 14 days (AL1 cells) following treatment.

Statistics

Basic statistical comparisons between control and experimental groups were conducted using JMP software (SAS, Cary, NC) to report standard deviation, standard error of the mean, and to conduct an independent t-test of unequal variance. T-tests were used to measure differences in cell proliferation in the dermis and epidermis of FTE skin wounds, differences in fibroblast numbers in the regenerating dermis, and differences among the percent of AL1 and hADF cells in various stages of the cell cycle.

A two-way ANOVA was used to determine if there were any significant differences in apoptosis among treated and untreated skin wounds depending on the day of regeneration, the experimental group, and the interaction between day and group. Alpha was set at 0.05.

RESULTS

In order to investigate the effect of beryllium on regenerative ability, we first sought to replicate C. S. Thornton's original experiments showing that a short beryllium exposure completely inhibited limb regeneration (see Methods) (Thornton, 1949, 1950, 1951). Replicating the originally published parameters and substituting juvenile axolotls (*Ambystoma mexicanum*) for *Ambystoma opacum* larvae, we found that limb regeneration was severely perturbed, but not completely inhibited, in response to beryllium nitrate (BeN) exposure (Figure 1). Examining control limbs after amputation, we found that a blastema formed in all animals and progressed through the normal stages of limb regeneration, ultimately leading to complete regeneration of a normal stylopod, zeugopod and autopod (Figure 1A-C). In contrast, BeN treated limbs formed a small edema at the amputation plane that persisted until control limbs had already formed digits (Figure 1D). Analyzing BeN treated limbs 98 days after injury (D98), we observed very small, mispatterned limbs that were well-vascularized (Figure 1E). By D200, some melanocytes had migrated distally, but limbs remained heteromorphic (Figure 1F). While the presence of digits and the number was variable across all BeN treated animals, melanocyte migration was always disrupted (Figure 1E-F). Similar to previous studies, we found that the degree to which limb regeneration was inhibited was dependent on the size of the animal and the concentration of beryllium; larger animals required a higher molar concentration to inhibit limb regeneration (data not shown). We followed some animals for up to two years after BeN exposure and observed no adverse health affects. Animals continued to grow and reproduce, which supported previous assertions that beryllium inhibited regeneration locally, rather than altering whole organism physiology (Thornton, 1949).

Seeking to remove the complexity of limb patterning in order to investigate how beryllium might inhibit regeneration, we turned to a full-thickness skin defect. Our previous work showed that adult paedomorphic axolotls could completely regenerate a 4 mm full-thickness excisional skin wound in 80 days (Seifert et al., 2012) and we observed a similar time course during our experiments (Figure 2A, C, E, G). We compared BeN treated skin wounds to control wounds and noted several important effects (Figure 2B, D, F, H). D14 BeN treated wounds showed a similar response to BeN treated limbs and were notable for a lack of pigment cells migrating into the wound, persistent presence of edema in the wound bed and increased wound area compared to controls (Figure 2B). Tracking wounds over time we noted a difference in wound area between treatment and control groups beginning at D14 (Figure 2A, B). By D21, control wounds were significantly smaller than BeN treated wounds ($9.93 \pm 0.91 mm^2$ and $28.77 \pm 2.82 mm^2$ respectively, $t = 6.20$, $p < 0.002$; n=5 per group). In fact, wound area in BeN treated wounds had more than doubled compared to the original wound area (original wound = $12.57\ mm^2$ vs. D21 BeN wound area = $28.77 \pm 2.82 mm^2$). Whereas the original wound was difficult to visualize at D64 in control samples, treatment wounds were still visible at this time point, but became harder to detect by D80 (Figure 2E-H). These results suggested that BeN exposure inhibited wound contraction following injury.

We next examined the cellular structure of healing wounds and found that keratinocytes re-epithelialized treatment and control wounds in 24 hours (data not shown). A thin layer of keratinocytes and Leydig cells covered all wounds within 24 hours of injury and wounding elicited a typical hemostatic response (Figure S1). While blood cells were present in treatment and control wounds, a large number of erythrocytes

and plasma persisted in BeN treated wounds until D21 (Figure 2B, D and Figure 3). In parallel with greater numbers of erythrocytes, ECM deposition was strongly inhibited by BeN treatment. While we detected collagen in control wounds beginning at D14, collagen deposition was not detected in treatment wounds until after D21 (Figure 3). In D42 control wounds, the regenerating dermis began stratifying into an upper stratum spongiosum and lower stratum compactum, and new glands were evident regenerating from the epidermis (Figure 3). By D80, skin in control wounds had completely regenerated and resembled unwounded skin (Figure 3). In contrast, D42 BeN treated wounds developed a dense dermal ECM layer associated with the basement membrane and no regenerating glands were present (Figure 3). Surprisingly, D80 wounds in BeN treated skin resembled D42 control wounds, whereby the collagen-rich dermal layer began subdividing and new glands were evident descending from the epidermis (Figure 3). At D139, there was little noticeable difference between treatment and control wounds. Together, these data demonstrated that BeN exposure delayed, but did not inhibit skin regeneration.

Our observation of reduced collagen deposition following BeN treatment led us to ask whether other components of the extracellular matrix normally deposited during skin regeneration were similarly affected (Seifert et al., 2012). Analyzing wound bed tissue at D14, we found that fibronectin-1 (FN1) and tenascin-C (TNC) were deposited throughout the regenerating dermis (Figure 4). We also used Alcian blue to detect glycosaminoglycan (GAG) production and found it present throughout the wound bed in control skin (Figure 4). In contrast to control treated wounds, FN1 and TNC were barely detectable in BeN treated wounds (Figure 4). Similarly, GAGs were not present in the

wound bed of the treatment group (Figure 4) at D14. Together with our histological observations, these results indicated that BeN inhibits ECM deposition (directly or indirectly) and this is associated with a delay in the normal time course of skin regeneration.

A lack of ECM production in BeN treated wounds suggested three hypotheses: (H1) a persistent inflammatory response prevented progression to a regenerative response or (H2) fibroblasts were not present and persistent in the wound or (H3) fibroblasts were not migrating into the wound bed. We first sought to test whether BeN treatment increased cellular inflammation in the wound bed. We assessed leukocyte numbers using an antibody to L-plastin, a pan-leukocytic marker (Jones et al., 1998; Seifert et al., 2012). Calculating percent L-plastin+ cells in the wound bed at D7, we found significantly fewer cells in BeN treated versus control wounds ($0.20 \pm 0.17\%$ and $3.09 \pm 0.49\%$ respectively, $t = -6.10$, $p < 0.003$) (Figure 5). This data showed that BeN did not stimulate increased inflammatory cell influx into dorsal skin wounds, although erythrocytes and plasma were found to persist longer in the wound bed in BeN treated wounds.

Dermal fibroblasts are the primary cell type involved in blastema formation (Gardiner et al., 1986, Muneoka et al., 1986) and are responsible for producing ECM during regeneration (Asahina et al., 1999; Calve et al., 2010; Gulati et al., 1983; Onda et al., 1990; Seifert et al., 2012). The relative absence of ECM proteins in the wound bed of BeN treated wounds suggested fibroblasts might be absent from the wound bed, either because they failed to migrate into the wounds or because they failed to survive due to BeN exposure. We tested multiple commercially available antibodies that label mammalian fibroblasts (PDGFR-alpha (R+D Systems), vimentin (Sigma-Aldrich), 40E-C

(Developmental Studies Hybridoma Bank) for their reactivity to axolotl dermal fibroblasts. Although we used our robust immunohistochemical protocol and tested a number of variables, including paraffin sections (with various antigen retrievals) and frozen tissue sections, we were unable to reliably label axolotl fibroblasts (data not shown). To circumvent this technical limitation, we took advantage of a transgenic axolotl line in which all cells constitutively express GFP (Sobkow et al., 2006). We transplanted skin (epidermis and dermis) from axolotls that constitutively express GFP in all cells into WT hosts (whose cells do not express GFP) in order to track fibroblast presence and migration into injured tissue (Figure 6A). We counted GFP+ cells at D14 when fibroblasts are normally observed in the wound bed and ECM molecules are readily detectable (Figure 3 and 4). We found 5.66 ± 1.9% and 0.33 ± 0.11% GFP+ cells in control and BeN treated wounds respectively ($t = -6.44$, $p < 0.0001$, 2-tailed t-test) (Figure 6B-D). This confirmed that few fibroblasts were present in BeN treated wounds and suggested that BeN might induce cell death or restrict, either directly or indirectly, the migratory ability of fibroblasts into the wound. We performed a TUNEL assay on tissue harvested from control and BeN treated wounds at D1, D3, and D7 to test whether BeN treatment induced cell death in local fibroblasts and found no significant difference between groups at any time point ($F = 0.2018$, $p = 0.9583$, two-way ANOVA) (Figure 7A-C). Thus, our data showed that BeN treatment primarily affected fibroblast migration and does not induce cell death in local fibroblasts or in other wound bed cells.

While our transplant experiment demonstrated that fibroblasts failed to move into the wound bed, we could not rule out that beryllium exposure might affect production of a chemotactic factor either from the epidermis or other cells within the wound bed. To

directly test the affect of BeN on cell migration, we cultured axolotl AL1 cells (an immortalized dermal fibroblast line) and exposed them to BeN. First we tested the cytotoxicity of three concentrations of BeN based on our 100mM *in vivo* treatment (i.e., 1mM, 10mM and 100mM). Using Trypan Blue to detect dead cells, we determined 10mM BeN to be an optimal treatment concentration where minimal cell death occurred in response to treatment. To assess migratory ability *in vitro* we created an artificial wound using a round sterile applicator in the center of each well of a 12-well plate (Figure 8). Following cells every 24 hours we noted that control (untreated) cells began migrating into the *in vitro* wound on D2. By D14 large numbers of untreated cells had migrated into the wound center (Figure 8). In stark contrast, by D14 we found that few fibroblasts had migrated into the circular wound (Figure 8). Because we conducted the assay at ~70-80% confluency, we assessed confluency outside the scratch at D14 and found that cells were confluent in control and treatment groups (Figure 8). Together, these data show that axolotl fibroblasts treated with BeN exhibit greatly reduced migratory behavior compared to control cells without inhibiting cell division.

We next asked if our findings could be expanded to mammalian cells and asked if BeN treatment reduced the migratory ability of human dermal fibroblasts (hADF cells) (Figure 9). We performed the same *in vitro* assay as above and followed hADF cells every 12 hours (Figure 9). Similar to axolotl AL1 cells, we found that a 10mM treatment with BeN reduced the migration of cells into scratch wounds. Untreated hADF cells successfully migrated and completely filled an *in vitro* wound by 96 hours (Figure 9). Few BeN treated cells migrated into the scratched area by 96 hours and the area remained largely uninhabited by cells even 15 days after treatment (Figure 9 and data not shown).

We also noted a tendency of BeN treated cells to detach from the plastic and remain alive (Figure 9). Examining cells outside of the scratched areas, we noted that while control wells reached 100% confluency, cells in treated wells remained at approximately 70% confluency suggesting limited cell growth (Figure 9).

Although it appeared that axolotl fibroblasts continued growing after BeN treatment, the failure to reach confluency in hADF cells suggested BeN might affect cell cycle progression differently in various cell types. Thus, we used flow cytometry to calculate the relative fraction of cells present in each phase of the cell cycle in order to gain insight into how BeN might affect cell cycle progression. We first examined AL1 cells. Following control or BeN treatment, we allowed AL1 cells to continue cycling for 48 hours (equal to at least one complete cell cycle) (Maden, 1978; Wallace and Maden, 1976), labeled cells with propidium iodide, and then sorted cells based on their DNA content (Table 1). Our analysis indicated that BeN treatment led to a small, but significant increase in the percentage of cells in S-phase and G2/M-phase (Table 1). The percentage of cells in G0/G1, however, was not different between treatment and control. We next analyzed the effect of BeN treatment on proliferation of the regenerating limb *in vivo* with EdU during early blastema, mid blastema, and palette stages (Figure S2). We found a reduction in the proliferative index of the BeN treated group during the blastema stages (early blastema: control = 20.03 ± 2.59%, treatment = 5.74 ± 1.37%, $t = -4.89$, $p < 0.001$; mid blastema: control = 24.49 ± 0.75%, treatment = 14.71 ± 2.86%, $t = -3.26$, $p < 0.01$), but a recovery of proliferation at a later stage (palette: control = 24.58 ± 3.29%, treatment = 26.40 ± 3.63%, $t = 0.37$, $p = 0.71$), suggesting either BeN was only temporarily affecting fibroblast proliferation, or the lack of fibroblasts during the early

stages of limb regeneration was skewing proliferation counts. Interestingly, when we analyzed keratinocyte proliferation, we found no difference in the percent of BrdU+ cells comparing BeN treated epidermis and control epidermis at either 7 days after amputation (control = 10.56 ± 3.46%, treatment = 7.91 ± 1.77%, t = -0.78, p = 0.447) or 14 days following amputation (control = 18.15 ± 2.22%, treatment = 24.63 ± 2.29%, t = 2.06, p = 0.048) (Figure S3). Analyzing hADF cells *in vitro*, we found that BeN had a different effect on the mammalian cell cycle (Table 1). In contrast to AL1 cells, we found a significant decrease in the percentage of cells in S-phase and G2/M, whereas the percentage of cells in G0/G1 increased by 20% (Table 1). Together, this data suggests that BeN effects cell cycle progression differently in axolotl versus human cells.

DISCUSSION

Salamanders are known to regenerate their skin and limbs following injury. Many of the molecular mechanisms that define these processes remain to be discovered. In this study, we confirmed that beryllium nitrate (BeN) grossly altered regenerating *Ambystoma mexicanum* (axolotl) limbs. Furthermore, we demonstrated that a similar application of BeN to full thickness skin injuries delayed, but did not inhibit skin regeneration and that BeN affected the ability of fibroblasts to migrate sufficiently into the wound bed. This in turn resulted in little to no extracellular matrix deposition at the injury sites. These results support the idea that fibroblasts must migrate into the injury site and that their presence is necessary for epimorphic regeneration. This is born out of observations that fibroblasts are necessary to establish a blastema, in the case of limb regeneration, or deposit and remodel the wound bed ECM in the case of skin regeneration. Thus, our study provides a cellular mechanism underlying beryllium's inhibitory effect on regeneration in salamanders. Interestingly, our results also show that despite inhibiting local fibroblasts from migrating into skin injuries, additional fibroblasts from the periphery eventually arrive in the wound bed to regenerate the dermis.

Charles Thornton (1949, 1950, 1951) showed that limb regeneration of *Ambystoma opacum* larvae could be completely inhibited with the application of BeN to a limb stump without any adverse short-term effects to the rest of the organism. Our experiments treating axolotl larvae with BeN produced stunted, heteromorphic limbs with few pigment cells and missing digits. There are several explanations for our finding that limb regeneration was not completely inhibited. First, complete versus partial inhibition could be attributed to species differences as the original studies used *Ambystoma opacum* larvae, although this is unlikely in our opinion given that beryllium inhibits regeneration

in other *Ambystoma* species, newts and *Xenopus* larvae (Mescher et al., 2013; Scheuing and Singer, 1957; Thornton, 1949, 1950, 1951; Tsonis et al., 1991). Second, the effect of BeN as a regeneration inhibitor was reported to be size dependent (for a given concentration), with reduced effects observed on larger organisms (Thornton, 1949). The axolotl larvae used in the present experiments were larger (7-9 cm) than the *A. opacum* in Thornton's experiments (3-4 cm and 6-7 cm) and thus it is likely that a similar concentration of BeN (N/7) was insufficient to achieve complete inhibition. It is also possible that beryllium may affect larval limbs more completely.

Although previous studies showed that beryllium could completely inhibit limb regeneration in larval salamanders (Needham, 1941; Scheuing and Singer, 1957; Thornton, 1949; Tsonis et al., 1991), only one study has proposed a possible molecular mechanism which involves phosphatidylinositol phosphate (PIP) metabolism (Tsonis et al., 1991). Inositol 1,4,5-trisphosphate (IP_3) production was shown to rapidly increase following limb amputation and then rapidly decrease within 5 minutes (Tsonis et al., 1991). $BeSO_4$ exposure caused a 22% decrease in PIP metabolism 30 seconds after amputation, although $BeSO_4$ exposure at later time points had no affect on PIP metabolism. While this study suggested that $BeSO_4$ exposure inhibits regeneration by producing an inhibitory effect on cell proliferation because IP_3 production has been linked to cell cycle activation and proliferation (Berridge, 1987), the authors provided no data on cell proliferation. Scheuing and Singer's work (1957) using newts also seems to provide an alternative to the proposed PIP mechanism whereby fully formed blastemas were directly infused with similar concentrations of BeN and regeneration was inhibited. Because the treatment occurred many days after injury when IP_3 levels are low, it seems

unlikely that beryllium exerts its inhibitory effect through PIP metabolism. However, it is possible that beryllium has multiple effects on regeneration, both immediately after amputation (PIP-IP3 metabolism) and at a later time (BeN infusion of blastemas). We did find a small decrease in the proliferative index of cells beneath the epidermis at later time points, although we found no effect on keratinocytes. Given our findings linking BeN exposure to a migration defect, it is likely that the decrease in cell proliferation is a consequence of few cells migrating into the wound bed. Interestingly, evidence exists linking PIP metabolism to cell migration *in vitro* (Oppelt et al., 2012). Further studies are required to determine if PIP metabolism is linked to reduced cell migration in salamander cells.

Beryllium has been explored extensively in the context of chronic berylliosis disease whereby inhalation of beryllium dust causes an acute chronic inflammation of the lungs (Newman, 2007). In mammals, this occurs via an acute immune response where beryllium is identified by the major histocompatibility complex and antigen-presenting cells that themselves stimulate the proliferation and accumulation of CD4+ helper T cells, forming granulomatous tissue in the bronchoalveolar lavage of the lungs (Saltini et al., 1989). Extended beryllium exposure to the skin also leads to an accumulation of CD4+ cells at the point of contact (Fontenot et al., 2002; Saltini et al., 1989). Thus, depending on varying levels of susceptibility, the adaptive immune response in mammals is responsible for the symptoms associated with chronic berylliosis disease. Interestingly, while much of the T-cell receptor complex has remained conserved between amphibians and mammals (Fellah et al., 1993), functional differences have occurred, specifically in the V-beta region of the T-cell receptor (Fellah et al., 1994). Generally, the immune

response of ectothermic organisms is mild relative to the exacting response of the mammalian immune system and lacks the organization or memory provided by B-lymphocytes, which are absent in axolotls (Hsu, 1998). A recent study treated larval *Xenopus laevis* with a beryllium solution and showed that beryllium increased the inflammatory response and this attenuated regenerative ability (Mescher et al., 2013). In contrast, our results in salamanders exposing limb amputations and skin wounds to BeN suggested that a sensitized immune system is not present following BeN exposure and did not account for the lapse in regeneration. While we observed an edema composed of plasma and erythrocytes consistent with a prolonged hemostatic response, few inflammatory leukocytes were present at the treatment site. Admittedly, no reagents exist to detect T-cells in salamanders so we could not assay for increased infiltration of these cells, and more importantly, T-cell polarization. The depletion macrophages have been shown in axolotls to inhibit limb regeneration (Godwin et al., 2013). While we cannot rule out the effect of macrophage reduction on regeneration, we infer that the effect of this deficit is playing a minor role when viewed in the context of our results and the role of fibroblasts in regeneration. Taken together, the data suggests that beryllium can act as an immunostimulatory agent in frogs and mammals, but that immune stimulation does not underlie the inhibitory effect of beryllium on regeneration in salamanders.

The dermal cell population has been reported to play a large role in limb regeneration by contributing up to 78% of the cells to the blastema (Muneoka et al., 1986). We showed that BeN reduces the ability for fibroblasts to migrate *in vivo* and *in vitro*. Despite poor fibroblast migration during the early stages of regeneration in response to BeN, some fibroblasts eventually migrated into the injured areas. As a result,

we observed a delay in skin regeneration, rather than an inhibition. Where these additional cells come from is a mystery, although it is possible that there is a fluid exchange of fibroblasts within the dermis and that given enough time, unaffected fibroblasts eventually infiltrate the wound site in high enough numbers to produce new ECM and regenerate the dermis. In the context of limb regeneration, the appearance of a few digits and carpals suggests that either a very small blastema formed or that a small accumulation of cells differentiated into the most distal structures. It remains unclear whether beryllium permanently affects the fibroblasts or if the effect eventually subsides, however, it is clear that the effect is sufficient to significantly alter limb regeneration and delay both skin and limb regeneration.

One of the major concern of exposing tissue or cells to a highly reactive element such as beryllium is the risk of toxicity to basic cellular processes (e.g., DNA synthesis, cell proliferation, cell death, transcription, etc.). We addressed these concerns by quantifying DNA synthesis and by fluorescently labeling dying cells. Beryllium toxicity has been cited as a caspase-dependent apoptotic pathway (Pulido and Parrish, 2003). We were able to assess apoptosis through TUNEL labeling and found that BeN exposure did not increase the number of apoptotic cells *in vivo*. Some studies suggest that beryllium has an antagonistic effect on cellular proliferation (Skilleter et al., 1983; Witschi, 1968). We did observe a small and transient reduction in cell proliferation in wound fibroblasts and mesenchymal cells beneath the epidermis, however fewer fibroblast cells were present following treatment. Since we calculated the proliferative index based on cell density this finding suggests that the observed reduction of proliferation was caused by a shift in the ratio of fibroblasts to transient, non-proliferative erythrocytes and leukocytes.

Beryllium affects cell cycle progression, however the magnitude of its effect *in vivo* was likely overestimated. Interestingly, proliferation of the epidermis was unaffected by BeN treatment which implies a targeted, cell-specific interaction rather than a ubiquitous cytotoxic response. Our *in vitro* cell cycle analysis showed a small but significant increase in the number of cells in S-phase and a decrease in the number of cells in G2/M-phase following BeN treatment which suggests a defect at the S/G2 checkpoint. When we consider our *in vivo* and *in vitro* data together it appears as if BeN exposure also affects cell cycle progression, although as a secondary effect to cell migration since many cells present at the injury site are proliferating.

We also conducted a cell cycle analysis on an hADF cell line and found that our results closely mirror those found for rat liver cells exposed to beryllium (Skilleter et al., 1983). We saw a significantly higher percentage of cells in G1-phase, and a significantly lower percentage of cells in S-phase and G2/M-phase. Thus, in mammalian cells, beryllium exposure results in a more acute, disruptive response to cell cycling compared to axolotl cells in combination with its effect on fibroblast migration.

Thus, our study shows that beryllium appears to affect endogenous tissue regeneration in two distinct ways: first, through a disruption of cell migration and second, through a small, transient interruption of cell cycle progression. It remains unclear if BeN operates as a mechanical impairment of the cell's motility systems (extension and reduction of cytoskeleton or integrin binding) or a sensory impairment of surface receptors and cell signaling machinery. Our experiments have brought to light an interesting phenomenon with potential real-world applications in the ongoing effort to improve clinical efforts to antagonize scarring. Scar formation in mammals results from

the production of excessive, densely packed collagen fibers following injury or in response to fibrotic disease. Because BeN exposure appears to limit fibroblast migration in a cell-type specific manner, an indirect outcome is a reduction in fibrosis. While this result reduced regenerative ability in a salamander, the *in vivo* effect in a mammalian injury may result in decreased scar formation. Future studies could be conducted to demonstrate the efficacy of low-dose BeN application to mammalian skin injuries, particularly those prone to high levels of scarring such as frostbite or burn. However, given the propensity of beryllium to elicit T-cell polarization, the immunostimulatory effects of beryllium may overwhelm any potential benefits as an anti-fibrotic. In this respect, beryllium appears to offer a unique tool to tease apart the intricacies of vertebrate regeneration and scarring.

TABLES

Table 1. Flow cytometric analysis of the cell cycle revealed that beryllium nitrate treatment produced an increased percentage of cells in S-phase and G2/M had an effect on the S/G2 transition in AL1 cells and on the G1/S phase transition in hADF cells.

AL1 Cell Cycle Analysis					
Cell Population (n=3)	**Control (avg %)**	**Control SEM (%)**	**BeN Treated 10mM (avg %)**	**Treatment SEM (%)**	**t-test (p)**
G0/G1	44.78	0.91	45.95	0.37	0.2977
S	34.31	0.56	39.16	0.64	0.0047
G2/M	20.91	0.36	14.89	0.31	<0.001
hADF Cell Cycle Analysis					
Cell Population (n=4)	**Control (avg %)**	**Control SEM (%)**	**BeN Treated 10mM (avg %)**	**Treatment CV (%)**	**t-test (p)**
G0/G1	52.78	0.37	72.42	0.62	<0.001
S	6.19	0.21	2.69	1.35	0.042
G2/M	41.67	0.45	24.89	1.62	<0.001

FIGURES

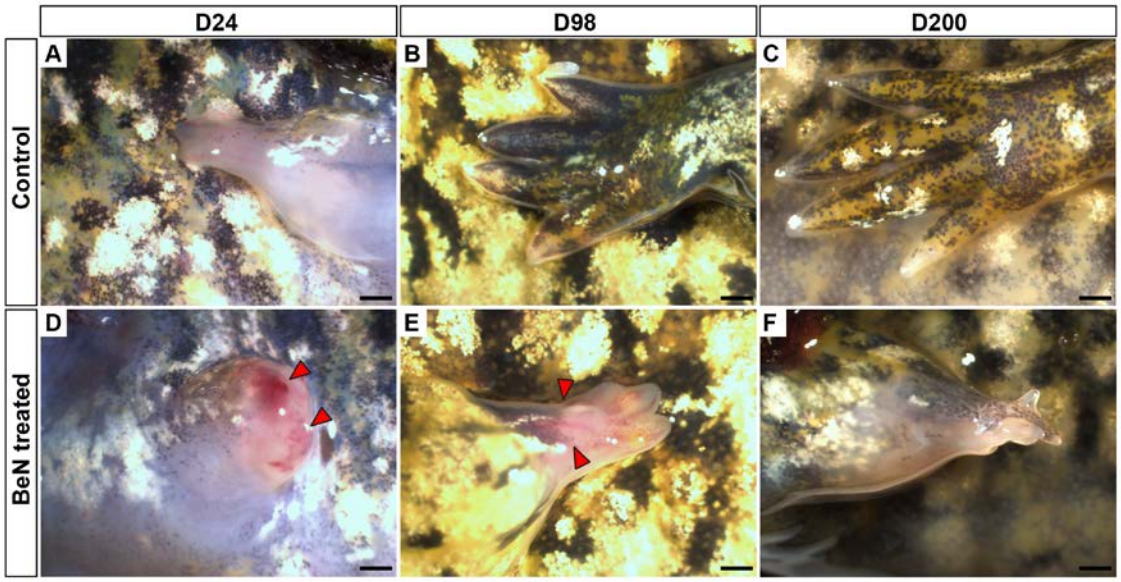

Figure 1. BeN treatment delays blastema formation and alters patterning during axolotl limb regeneration. Amputated limbs treated with BeN were imaged during regeneration alongside contralateral controls at D24 **(A, D)**, D98 **(B, E)**, and D200 **(C, F)** following injury. **(A)** D24, control limbs showed normal differentiation of the digits, while BeN treated limbs showed edema (arrows) with no gross signs of blastema formation **(D)**. **(B)** Untreated limbs had completely regenerated by 98 days. **(E)** D98 BeN treated limbs exhibited a delay in regeneration and patterning defects. Moreover, few melanocytes had migrated into the regenerate (arrows). Compared to control limbs at D200 **(C)**, BeN treated limbs showed permanent malformations including atypical digit formation and reduced melanocyte numbers **(F)**. Scale bar = 1mm.

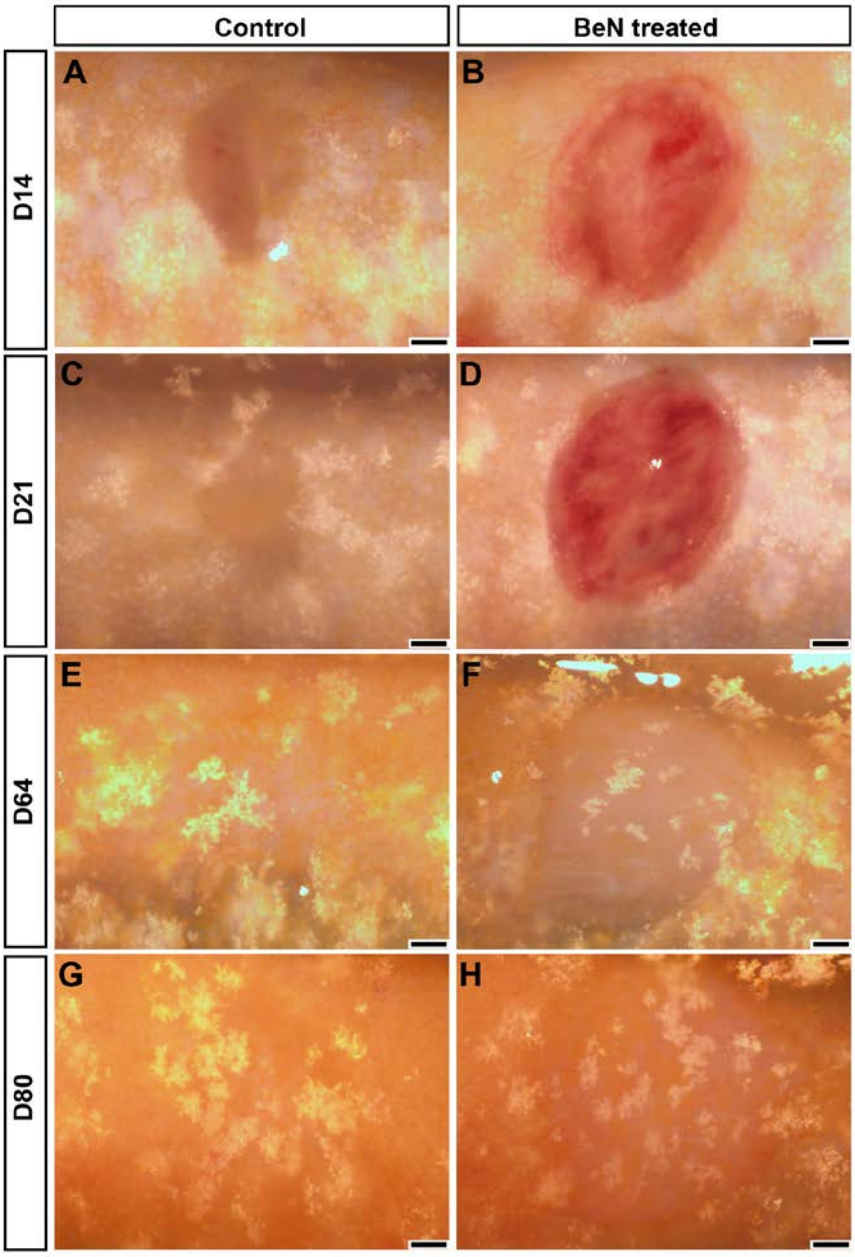

Figure 2. Beryllium nitrate inhibits wound contraction and delays pigment cell migration. (A-H) Comparison of full thickness excisional wound healing in control and BeN treated skin wounds in axolotls. Wounds were followed for 80 days. **(A, C)** Control wounds contracted during first 21 days. **(B, D)** BeN treated wounds expanded from initial biopsy area and retained large numbers of blood cells through D21. The average area of treated wounds at D21 was 3x larger than control. **(E-F)** Pigment cell (iridophore) migration was reduced in treated wounds. **(G-H)** D80 control wounds were indistinguishable from the surrounding unwounded tissue, while treated wounds maintained a clearly defined wound edge with dermal tissue and muscle still visible through the epidermis. Scale = 1mm.

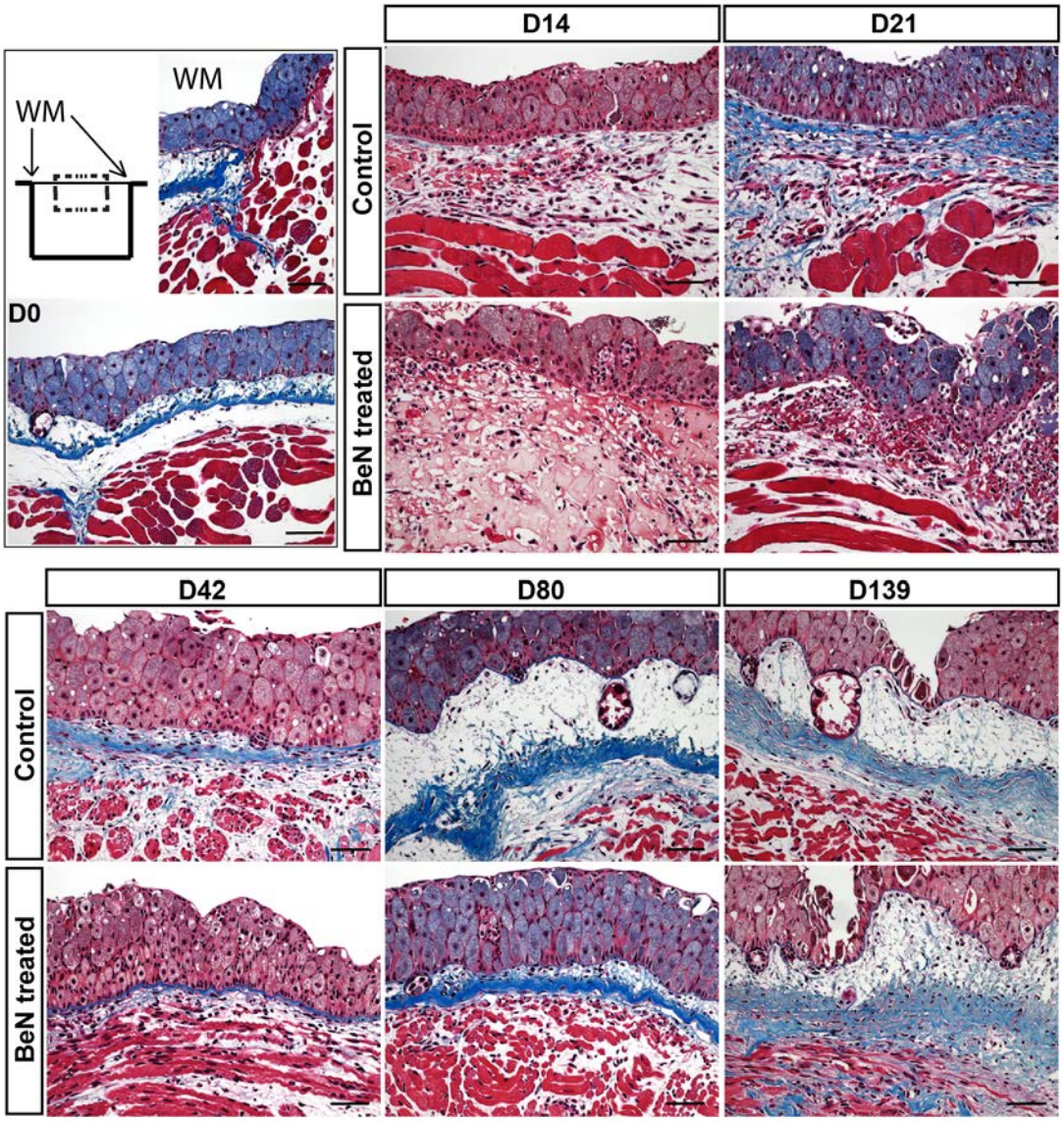

Figure 3. Beryllium nitrate exposure delays skin regeneration. Masson's trichrome stained sections comparing control and BeN treated full thickness excisional wounds in axolotls. Control wounds showed ECM deposition at D14. BeN treated wounds showed delayed ECM deposition until D42. ECM deposited at D42 was tightly bundled and localized near the basal lamina. Gland regeneration was apparent in control wounds at D42 and appeared at D80 in treated wounds. Full thickness skin (dermis and epidermis) in control wounds had completely regenerated by D80 and resembled unwounded tissue. Skin regeneration was delayed in treated wounds, with dermis and epidermis mostly regenerated by D139. Images represent center of the wound bed. Blue = collagen, red = muscle, purple = cytosol, black = nucleus. Scale = 100µm.

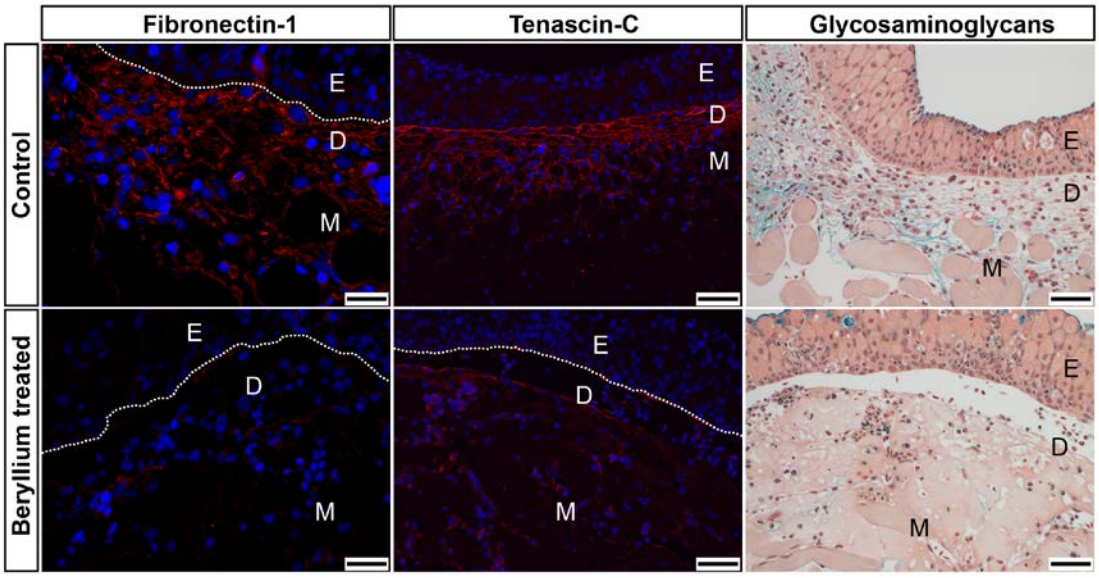

Figure 4. BeN inhibits early deposition of extracellular matrix (ECM) proteins in D14 axolotl skin wounds. Panels represent cross sections of full thickness skin showing epidermis (E), dermis (D) and muscle (M) in control and BeN treated wounds. Fibronectin-1, Tenascin-C and glycosaminoglycans (GAGs) are visible in the wound bed of controls, but are absent from BeN treated wounds. GAG presence was visualized with Alcian blue. Scale = 50µm (Fibronectin), 100µm (Tenascin-C and GAG).

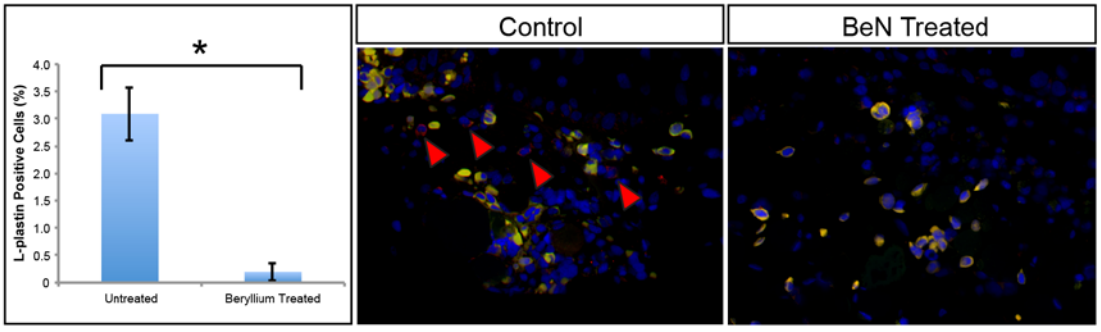

Figure 5. BeN treatment reduces leukocyte infiltration into skin wounds. Axolotl skin sounds were harvested at D7, and leukocytes were detected with the pan-leukocytic marker L-plastin. Control wounds contained significantly more L-plastin positive cells compared to BeN treated wounds ($t = -6.10$, $p < 0.003$). Red arrows indicate L-plastin positive cells in control wounds. Yellow cells are autofluorescing blood cells captured with the combination of a GFP and RFP filter.

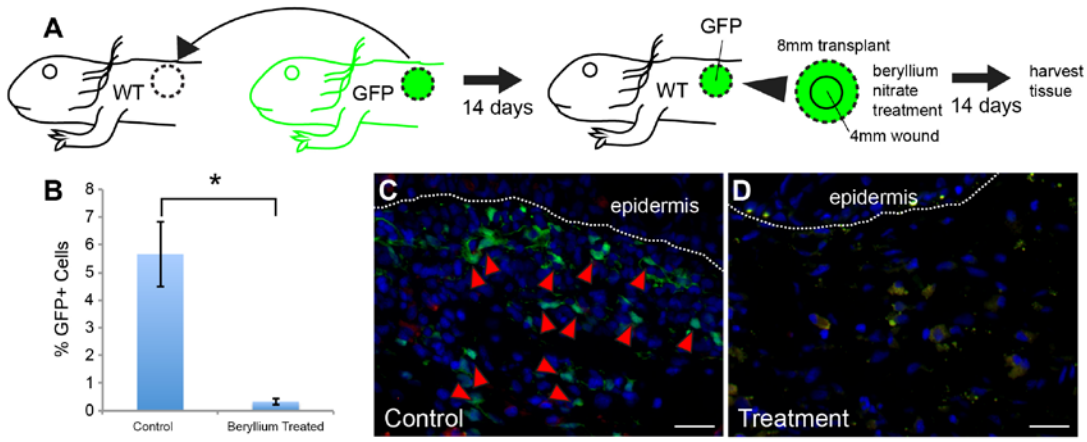

Figure 6. BeN reduces fibroblast migration into axolotl skin wounds. (A) Schematic depicts experimental paradigm for tracking GFP-labeled fibroblasts. 8mm skin biopsies containing epidermis and dermis were harvested from the dorsal flank of ubiquitously GFP-expressing axolotls (n=5) and transplanted to 8mm wound beds created on WT animals. Skin transplants were allowed to heal for 14 days after which a 4mm full thickness wound was made in the center of the transplant. BeN treatment occurred immediately following injury (see Methods). **(B-D)** Wound bed tissue was harvested at D14. **(B)** Control wounds had significantly more GFP+ cells compared to BeN treated wounds. **(C-D)** Red arrows indicate GFP+ cells. Few GFP+ cells were detected in BeN treated wounds. Erythrocytes that were auto-fluorescent at both red and green wavelengths and were not counted as GFP+. Scale = 50µm.

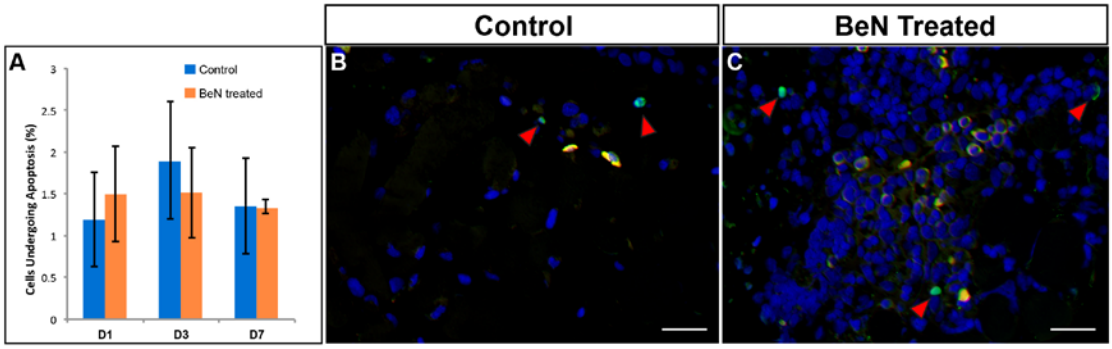

Figure 7. BeN treatment does not affect cell death *in vivo*. TUNEL assay was used to detect dying cells in axolotl wound bed tissue. **(A-C)** Percent dying cells were not different comparing control and BeN treated skin wounds across all time points examined (two-way ANOVA, F = 0.2018, p = 0.9583). Red arrows indicate TUNEL positive cells. Yellow cells are auto-fluorescent in both red and green wavelengths and thus were not counted as GFP+. Scale = 50µm.

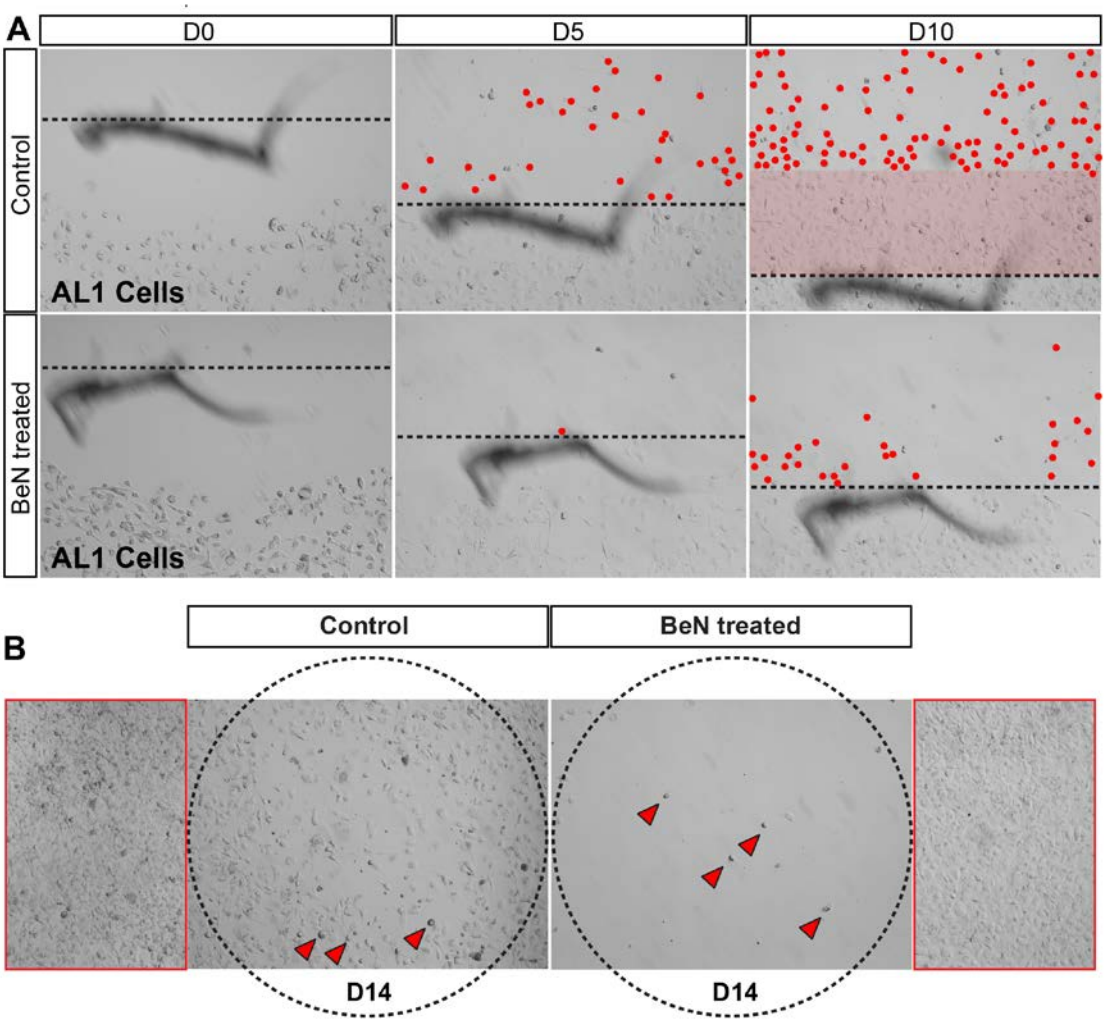

Figure 8. Beryllium nitrate reduces migratory capabilities of axolotl AL1 fibroblast cells *in vitro*. (A) Migration of AL1 fibroblasts across the inside edge (dotted line) of a circular scratch was tracked over the course of 10 days (red dots). The shaded box indicates an area >90% filled with cells. **(B)** BeN treatment inhibited migration of AL1 cells and reduced total migration distance. Dotted circle represents the original scratch area where untreated cells successfully migrated towards the center. Cell density was ~70-80% at treatment and cells in treated and control wells achieved confluency by D14 (red boxed areas). Red arrows indicate detached cells that were present in both treatment and control groups and did not stain with Trypan Blue (data not shown).

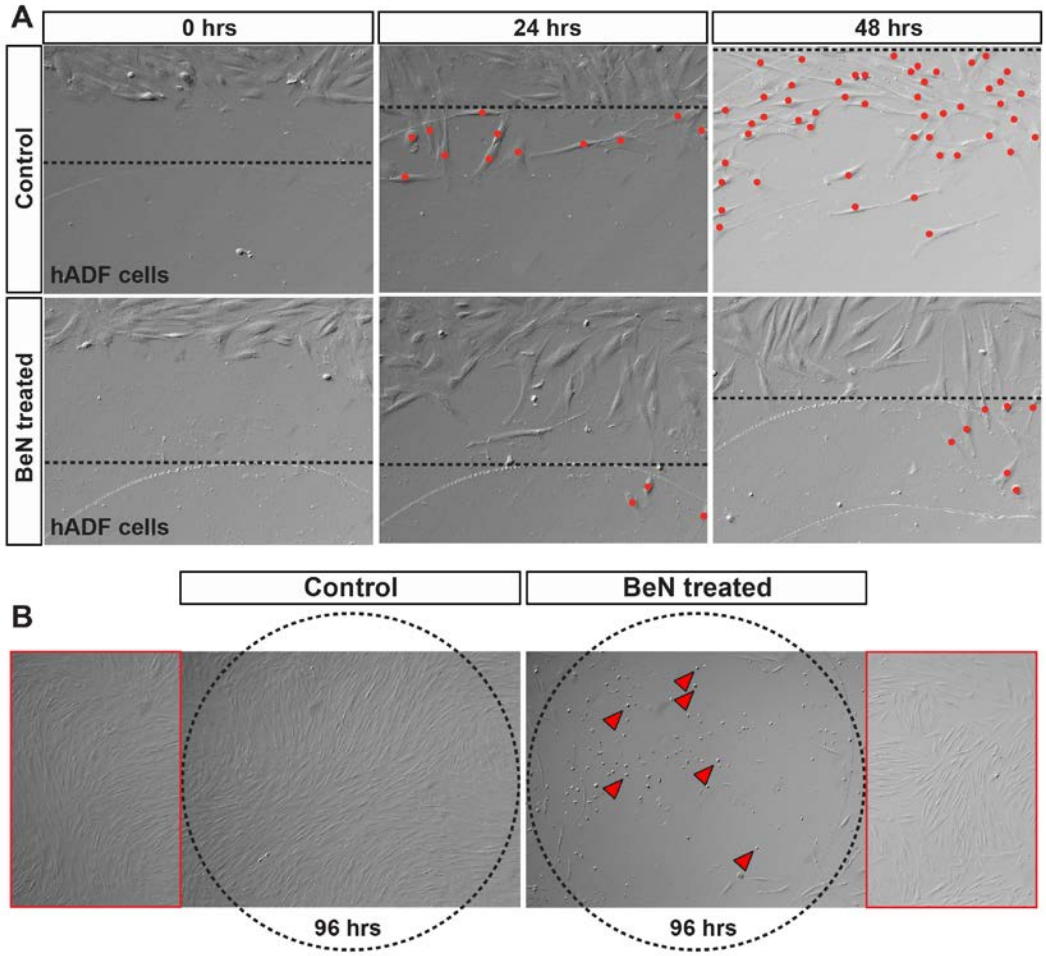

Figure 9. Beryllium nitrate reduces human dermal fibroblast migration *in vitro*. (A) Migration of human dermal fibroblast (hADF) across the inside edge (dotted line) of a circular scratch was tracked over 48 hours. Few cells treated with BeN migrated into the *in vitro* wound whereas control cells completely filled the wound after 96 hours **(B)**. BeN treatment reduced cell confluence of hADF cells outside of the immediate scratch area (red box). Red arrows show examples of cells in the treatment that have detached from the surface and did not stain with Trypan Blue (data not shown).

APPENDICES

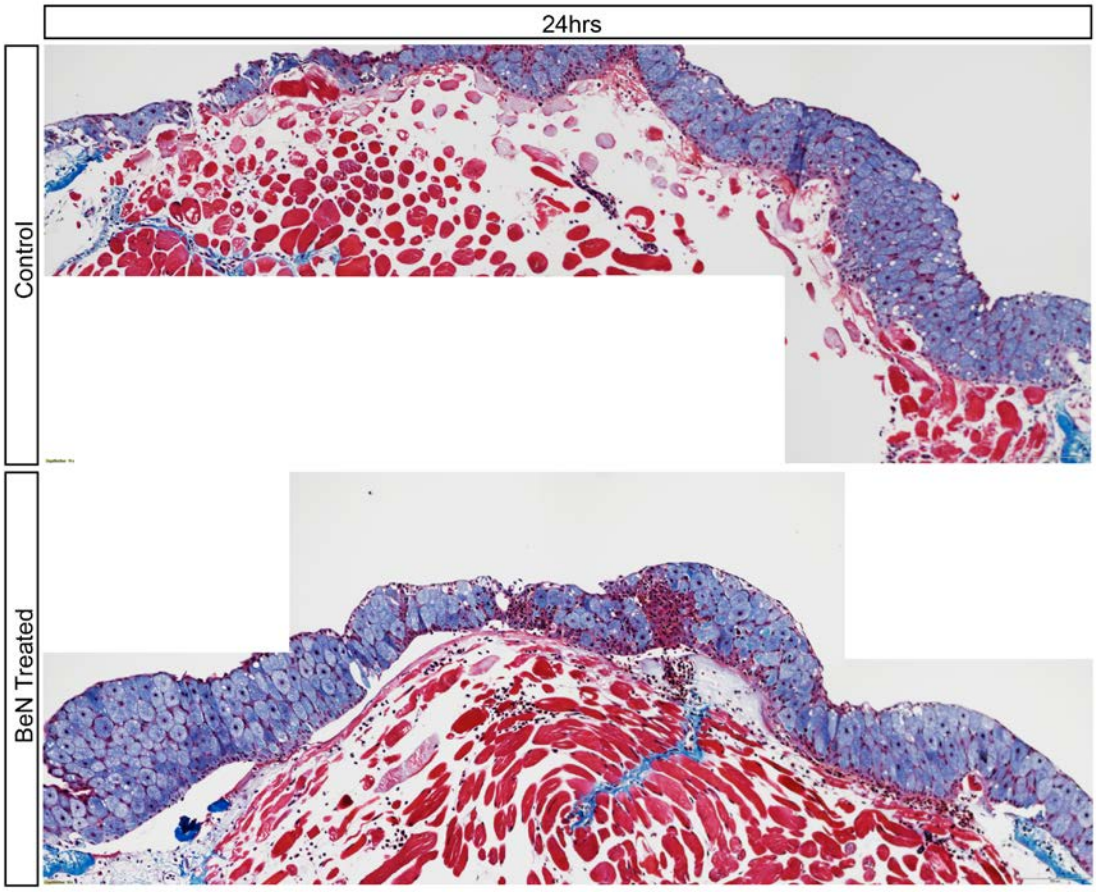

Figure S1. Epidermis migration and wound closure is unaffected by BeN treatment. Axolotl dorsal flank wounds treated with 100mM BeN were sectioned and stained with Masson trichrome. Epidermis covered the entire wound surface in both treatment and control after 24 hours. BeN treated wounds appeared to have portions of the epidermis in which densely packed erythrocytes interrupted the contiguous layer of Leydig cells.

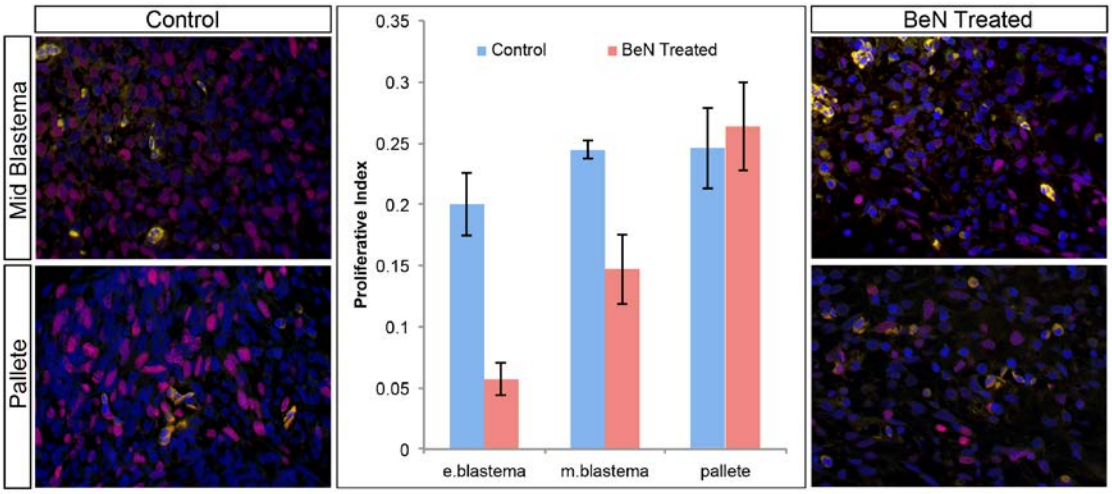

Figure S2. Percent EdU+ cells at early blastema, mid blastema, and palette stages of limb regeneration following treatment with BeN. Axolotl dorsal flank were wounds treated with 143mM beryllium nitrate, sectioned, and labeled with EdU. Two random fields of view were imaged and quantified. The treated limb bud had significantly fewer proliferating cells than the control in the early blastema (control = 20.03 ± 2.59%, treatment = 5.74 ± 1.37%, t = -4.89, $p < 0.001$) and the mid blastema (control = 24.49±0.75%, treatment = 14.71 ± 2.86%, t = -3.26, $p < 0.01$). The proliferative index was unchanged in the palette stage (control = 24.58 ± 3.29%, treatment = 26.40 ± 3.63%, t = 0.37, p = 0.71).

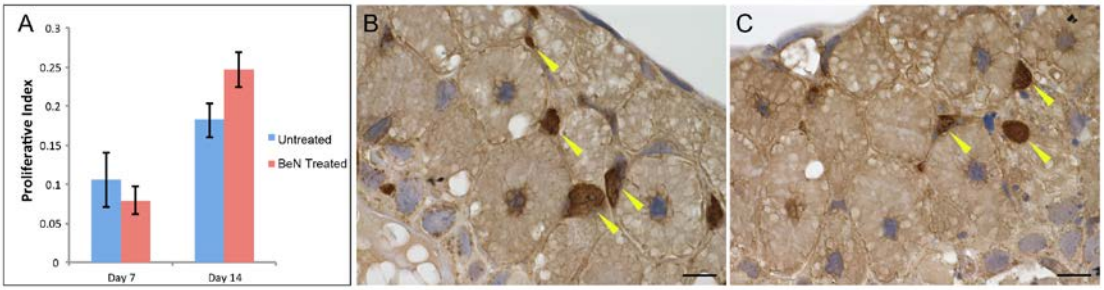

Figure S3. Proliferation of Leydig cells and keratinocytes of the epidermis was unaffected by BeN. (B, C) Proliferating cells, indicated by yellow arrows, had incorporated BrdU and were counted against the total epidermal cell population. **(A)** Proliferative indices were unaffected by the application of beryllium nitrate at both D7 (control = 10.56 ± 3.46%, treatment = 7.91 ± 1.77%, t = -0.78, p = 0.447) and D14 (control = 18.15 ± 2.22%, treatment = 24.63 ± 2.29%, t = 2.06, p = 0.048). Scale = 20µm.

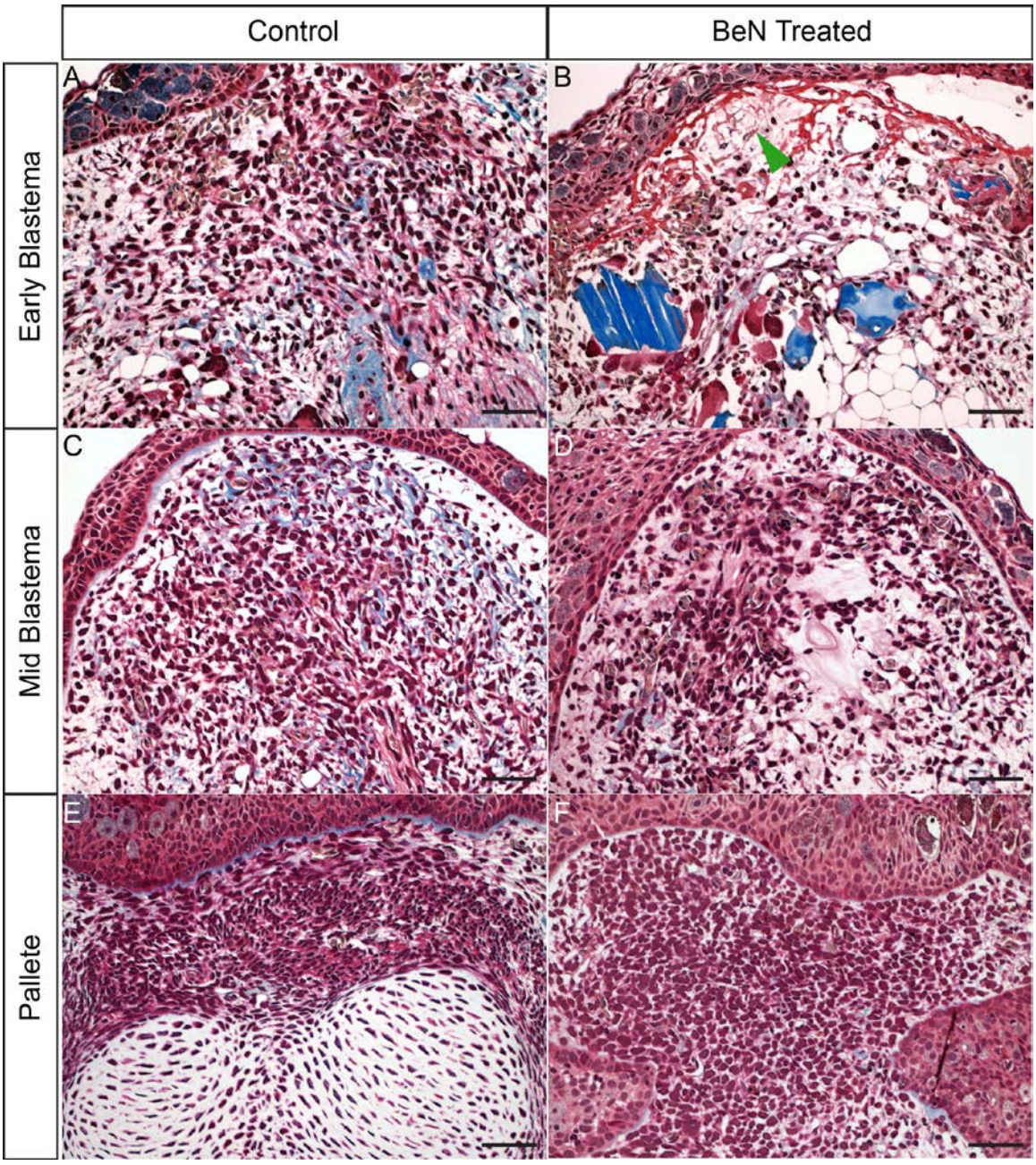

Figure S4. Beryllium delays ECM deposition and disrupts pattern formation in regenerating limb buds of the axolotl. (A, C) Extracellular matrix is visible among the undifferentiated blastema cell populations of the control regenerates. **(E)** Basal lamina can be seen beneath the epidermis, followed by signs of early limb patterning of the untreated palette. **(B, D, F)** Very little ECM is visible in the mesenchyme of the blastema or palette of the treatment group. **(B)** An edema is present in the sub-epidermal space of the treated early blastema (green arrow). **(F)** Visible lack of discernable patterning or basal lamina in the treated equivalent of a palette. **(A-F)** Treated blastemas have fewer cells present in the mesenchyme than their untreated counterparts. This disparity disappears during the later stages of limb regeneration. Scale = 100μm.

REFERENCES

Asahina, K., Obara, M., Yoshizato, K., 1999. Expression of genes of type I and type II collagen in the formation and development of the blastema of regenerating newt limb. Developmental dynamics 216, 59-71.

Berridge, M.J., 1987. Inositol trisphosphate and diacylglycerol: two interacting second messengers. Annual review of biochemistry 56, 159-193.

Brockes, J.P., 1987. The nerve dependence of amphibian limb regeneration. Journal of Experimental Biology 132, 79-91.

Bryant, S., Gardiner, D., 1989. Position-Dependent Growth Control and Pattern Formation in Limb Regeneration, in: Kiortsis, V., Koussoulakos, S., Wallace, H. (Eds.), Recent Trends in Regeneration Research. Springer US, pp. 377-390.

Bryant, S.V., 1976. Regenerative failure of double half limbs in Notophthalmus viridescens. Nature 263, 676-679.

Bryant, S.V., Endo, T., Gardiner, D.M., 2002a. Vertebrate limb regeneration and the origin of limb stem cells. International Journal of Developmental Biology 46, 887-896.

Bryant, S.V., Endo, T., Gardiner, D.M., 2002b. Vertebrate limb regeneration and the origin of limb stem cells. The International journal of developmental biology 46, 887-896.

Burnet, B.M., Liversage, R., 1964. THE INFLUENCE OF CHLORAMPHENICOL ON THE REGENERATING FORELIMB IN ADULT TRITURUS-VIRIDESCENS, AMERICAN ZOOLOGIST. AMER SOC ZOOLOGISTS 1041 NEW HAMPSHIRE ST, LAWRENCE, KS 66044, pp. 427-427.

Butler, E.G., Ward, M.B., 1967. Reconstitution of the spinal cord after ablation in adult Triturus. Developmental Biology 15, 464-486.

Calve, S., Odelberg, S.J., Simon, H.G., 2010. A transitional extracellular matrix instructs cell behavior during muscle regeneration. Dev Biol 344, 259-271.

Carlson, B.M., 1967. The histology of inhibition of limb regeneration in the newt, Triturus, by actinomycin D. J Morphol 122, 249-263.

Carlson, B.M., 1969. Inhibition of limb regeneration in the axolotl after treatment of the skin with actinomycin D. The Anatomical record 163, 389-401.

Carlson, B.M., 1974. Morphogenetic interactions between rotated skin cuffs and underlying stump tissues in regenerating axolotl forelimbs. Developmental Biology 39, 263-285.

Del Rincon, S.V., Scadding, S.R., 2002. Retinoid antagonists inhibit normal patterning during limb regeneration in the axolotl, Ambystoma mexicanum. The Journal of experimental zoology 292, 435-443.

Eguchi, G., Eguchi, Y., Nakamura, K., Yadav, M.C., Millan, J.L., Tsonis, P.A., 2011. Regenerative capacity in newts is not altered by repeated regeneration and ageing. Nat Commun 2, 384.

Fellah, J.S., Kerfourn, F., Charlemagne, J., 1994. Evolution of T cell receptor genes. Extensive diversity of V beta families in the Mexican axolotl. The Journal of Immunology 153, 4539-4545.

Fellah, J.S., Kerfourn, F., Guillet, F., Charlemagne, J., 1993. Conserved structure of amphibian T-cell antigen receptor beta chain. Proceedings of the National Academy of Sciences 90, 6811-6814.

Fontenot, A.P., Maier, L.A., Canavera, S.J., Hendry-Hofer, T.B., Boguniewicz, M., Barker, E.A., Newman, L.S., Kotzin, B.L., 2002. Beryllium skin patch testing to analyze T cell stimulation and granulomatous inflammation in the lung. Journal of immunology (Baltimore, Md. : 1950) 168, 3627-3634.
Gardiner, D.M., Muneoka, K., Bryant, S.V., 1986. The migration of dermal cells during blastema formation in axolotls. Developmental Biology 118, 488-493.
Godwin, J.W., Pinto, A.R., Rosenthal, N.A., 2013. Macrophages are required for adult salamander limb regeneration. Proceedings of the National Academy of Sciences of the United States of America 110, 9415-9420.
Gulati, A.K., Zalewski, A.A., Reddi, A., 1983. An immunofluorescent study of the distribution of fibronectin and laminin during limb regeneration in the adult newt. Developmental biology 96, 355-365.
Hsu, E., 1998. Mutation, selection, and memory in B lymphocytes of exothermic vertebrates. Immunological reviews 162, 25-36.
Jones, S.L., Wang, J., Turck, C.W., Brown, E.J., 1998. A role for the actin-bundling protein l-plastin in the regulation of leukocyte integrin function. Proceedings of the National Academy of Sciences 95, 9331-9336.
Lheureux, E., 1975a. Nouvelles donnees sur les roles de la peau et des tissues internes dans la regeneration du membre du triton Pleurodeles waltlii, Michah (amphibian urodele). Wilhelm Roux. Arch 776, 285-301.
Lheureux, E., 1975b. Régénération des membres irradiés dePleurodeles waltlii Michah.(Urodčle). Influence des qualités et orientations des greffons non irradies. Wilhelm Roux'Archiv für Entwicklungsmechanik der Organismen 176, 303-327.
Maden, M., 1978. Neurotrophic control of the cell cycle during amphibian limb regeneration. Journal of embryology and experimental morphology 48, 169-175.
Maden, M., Keeble, S., Cox, R., 1985. The characteristics of local application of retinoic acid to the regenerating axolotl limb. Wilhelm Roux's archives of developmental biology 194, 228-235.
Mchedlishvili, L., Epperlein, H.H., Telzerow, A., Tanaka, E.M., 2007. A clonal analysis of neural progenitors during axolotl spinal cord regeneration reveals evidence for both spatially restricted and multipotent progenitors. Development (Cambridge, England) 134, 2083-2093.
Mercader, N., Leonardo, E., Azpiazu, N., Serrano, A., Morata, G., Martínez-A, C., Torres, M., 1999. Conserved regulation of proximodistal limb axis development by Meis1/Hth. Nature 402, 425-429.
Mescher, A.L., Neff, A.W., King, M.W., 2013. Changes in the Inflammatory Response to Injury and Its Resolution during the Loss of Regenerative Capacity in Developing Xenopus Limbs. PloS one 8, e80477.
Muneoka, K., Fox, W.F., Bryant, S.V., 1986. Cellular contribution from dermis and cartilage to the regenerating limb blastema in axolotls. Developmental Biology 116, 256-260.
Needham, A.E., 1941. Some Experimental Biological Uses of the Element Beryllium (Glucinum). Proceedings of the Zoological Society of London A111, 59-85.
Newman, L.S., 2007. Immunotoxicology of beryllium lung disease. Environmental health and preventive medicine 12, 161-164.

Onda, H., Goldhamer, D.J., Tassava, R.A., 1990. An extracellular matrix molecule of newt and axolotl regenerating limb blastemas and embryonic limb buds: immunological relationship of MT1 antigen with tenascin. Development (Cambridge, England) 108, 657-668.
Oppelt, A., Lobert, V.H., Haglund, K., Mackey, A.M., Rameh, L.E., Liestøl, K., Oliver Schink, K., Marie Pedersen, N., Wenzel, E.M., Haugsten, E.M., Brech, A., Erik Rusten, T., Stenmark, H., Wesche, J., 2012. Production of phosphatidylinositol 5-phosphate via PIKfyve and MTMR3 regulates cell migration. EMBO reports 14, 57-64.
Pulido, M.D., Parrish, A.R., 2003. Metal-induced apoptosis: mechanisms. Mutation Research/Fundamental and Molecular Mechanisms of Mutagenesis 533, 227-241.
Qin, P., Cimildoro, R., Kochhar, D.M., Soprano, K.J., Soprano, D.R., 2002. PBX, MEIS, and IGF-I are potential mediators of retinoic acid-induced proximodistal limb reduction defects. Teratology 66, 224-234.
Salley, J.D., Tassava, R.A., 1981. Responses of denervated adult newt limb stumps to reinnervation and reinjury. The Journal of experimental zoology 215, 183-189.
Saltini, C., Winestock, K., Kirby, M., Pinkston, P., Crystal, R.G., 1989. Maintenance of Alveolitis in Patients with Chronic Beryllium Disease by Beryllium-Specific Helper T Cells. New England Journal of Medicine 320, 1103-1109.
Scheuing, M.R., Singer, M., 1957. The effects of microquantitles of beryllium ion on the regenerating forelimb of the adult newt, Triturus. The Journal of experimental zoology 136, 301-327.
Schotté, O.E., Butler, E.G., 1941. Morphological effects of denervation and amputation of limbs in urodele larvae. Journal of Experimental Zoology 87, 279-322.
Seifert, A.W., Monaghan, J.R., Voss, S.R., Maden, M., 2012. Skin regeneration in adult axolotls: a blueprint for scar-free healing in vertebrates. PloS one 7, e32875.
Singer, M., 1951. Introduction of regeneration of forelimb of the frog by augmentation of the nerve supply. Proc Soc Exp Biol Med 76, 413-416.
Singer, M., Flinker, D., Sidman, R.L., 1956. Nerve destruction by colchicine resulting in suppression of limb regeneration in adult Triturus. Journal of Experimental Zoology 131, 267-299.
Skilleter, D.N., Price, R.J., Legg, R.F., 1983. Specific G1-S phase cell cycle block by beryllium as demonstrated by cytofluorometric analysis. The Biochemical journal 216, 773-776.
Slack, J.M., 1983. Positional information in the forelimb of the axolotl: properties of the posterior skin. Journal of embryology and experimental morphology 73, 233-247.
Sobell, H.M., 1985. Actinomycin and DNA transcription. Proceedings of the National Academy of Sciences 82, 5328-5331.
Sobkow, L., Epperlein, H.H., Herklotz, S., Straube, W.L., Tanaka, E.M., 2006. A germline GFP transgenic axolotl and its use to track cell fate: dual origin of the fin mesenchyme during development and the fate of blood cells during regeneration. Dev Biol 290, 386-397.
Spallanzani, L., 1769. An essay on animal reproductions. T. Becket and PA de Hondt.
Thornton, C.S., 1943. The effect of colchicine on limb regeneration in larval Amblystoma. Journal of Experimental Zoology 92, 281-295.

Thornton, C.S., 1949. BERYLLIUM INHIBITION OF REGENERATION .1. MORPHOLOGICAL EFFECTS OF BERYLLIUM ON AMPUTATED FORE LIMBS OF LARVAL AMBLYSTOMA. Journal of Morphology 84, 459-&.
Thornton, C.S., 1950. BERYLLIUM INHIBITION OF REGENERATION .2. LOCALIZATION OF THE BERYLLIUM EFFECT IN AMPUTATED LIMBS OF LARVAL AMBLYSTOMA. Journal of Experimental Zoology 114, 305-333.
Thornton, C.S., 1951. BERYLLIUM INHIBITION OF REGENERATION .3. HISTOLOGICAL EFFECTS OF BERYLLIUM ON THE AMPUTATED FORE LIMBS OF AMBLYSTOMA LARVAE. Journal of Experimental Zoology 118, 467-&.
Tidball, J.G., Dorshkind, K., Wehling-Henricks, M., 2014. Shared signaling systems in myeloid cell-mediated muscle regeneration. Development (Cambridge, England) 141, 1184-1196.
Todd, T., 1823. On the process of reproduction of the members of the aquatic salamander. QJ Sci Lit Arts 16, 84-96.
Tsonis, P.A., English, D., Mescher, A.L., 1991. Increased content of inositol phosphates in amputated limbs of axolotl larvae, and the effect of beryllium. Journal of Experimental Zoology 259, 252-258.
Wallace, H., 1981. Vertebrate Limb Regeneration. John Wiley and Sons.
Wallace, H., Maden, M., 1976. The cell cycle during amphibian limb regeneration. Journal of cell science 20, 539-547.
Witschi, H., 1968. Inhibition of deoxyribonucleic acid synthesis in regenerating rat liver by beryllium. Laboratory investigation; a journal of technical methods and pathology 19, 67-70.
Yunis, A., 1989. Chloramphenicol toxicity: 25 years of research. The American journal of medicine 87, 44N-48N.

VITA

1. Place of birth:
   - Orlando, Florida

2. Educational institutions attended:
   - University of Florida, 2009-2013
     - Bachelor's of Science in Biology; Specialty in Biotechnology

3. Professional positions held:
   - Teaching Assistantship for the University of Kentucky Department of Biology, 2013-2015

4. Scholastic and professional honors:
   - Dean's list, 2009-2013
   - Graduated *cum laude*, 2013
   - MDI fellowship funding, June 2015, $165.00

5. Professional publications:
   - Cook, A. and Seifert, A. *Beryllium nitrate supports fibroblast migration as an essential component of skin and limb regeneration in axolotls.* Manuscript in preparation.

Adam Boyd Cook